

CardAIC-Agents: A Multimodal Framework with Hierarchical Adaptation for Cardiac Care Support

Yuting Zhang¹, Karina V. Bunting², Asgher Champs², Xiaoxia Wang^{2,3},
Wenqi Lu⁴, Alexander Thorley¹, Sandeep S Hothi⁵, Zhaowen Qiu⁶,
Dipak Kotecha^{2,3,7}, Jinming Duan^{1,8}

¹School of Computer Science, University of Birmingham, Birmingham, UK

²Department of Cardiovascular Sciences, University of Birmingham, Birmingham, UK

³NIHR Birmingham Biomedical Research Centre and West Midlands NHS Secure Data Environment, University Hospitals Birmingham NHS Foundation Trust, Birmingham, UK

⁴Department of Computing and Mathematics, Manchester Metropolitan University, Manchester, UK

⁵Department of Cardiology, Heart and Lung Centre, Royal Wolverhampton NHS Trust, Wolverhampton, UK

⁶College of Computer and Control Engineering, Northeast Forestry University, Harbin, China

⁷Julius Center, University Medical Center Utrecht, the Netherlands

⁸Division of Informatics, Imaging and Data Sciences, University of Manchester, Manchester, UK

Abstract

Cardiovascular diseases (CVDs) remain the foremost cause of mortality worldwide, a burden worsened by a severe deficit of healthcare workers. Artificial intelligence (AI) agents have shown potential to alleviate this gap via automated early detection and proactive screening, yet their clinical application remains limited by: 1) prompt-based clinical role assignment that relies on intrinsic model capabilities without domain-specific tool support; or 2) rigid sequential workflows, whereas clinical care often requires adaptive reasoning that orders specific tests and, based on their results, guides personalised next steps; 3) general and static knowledge bases without continuous learning capability; and 4) fixed unimodal or bimodal inputs and lack of on-demand visual outputs when further clarification is needed. In response, a multimodal framework, CardAIC-Agents, was proposed to augment models with external tools and adaptively support diverse cardiac tasks. Specifically, a CardiacRAG agent generated general plans from updatable cardiac knowledge, while the chief agent integrated tools to autonomously execute these plans and deliver decisions. To enable adaptive and case-specific customization, a stepwise update strategy was proposed to dynamically refine plans based on preceding execution results, once the task was assessed as complex. In addition, a multidisciplinary discussion tool was introduced to interpret challenging cases, thereby supporting further adaptation. When clinicians raised concerns, visual review panels were provided to assist final validation. Experiments across three datasets showed the efficiency of CardAIC-Agents compared to mainstream Vision-Language Models (VLMs), state-of-the-art agentic systems, and fine-tuned VLMs.

Introduction

Cardiovascular diseases (CVD) are the leading cause of mortality worldwide, with 17.9 million people deaths each year (Almeida et al. 2024). Notably, up to 80% of these deaths occur in low- and middle-income countries, where specialised care is limited (Bulto and Hendriks 2024), and this, combined with a global shortage of over 4 million

healthcare workers (Vedanthan and Fuster 2011), drives the demand for scalable and accessible cardiovascular care solutions. Recent advancements in large language models (LLMs) have achieved human-level performance; for instance, GPT-4o and Med-PaLM have outperformed clinicians on standardized assessments like the United States Medical Licensing Examination (Brin et al. 2023; Singhal et al. 2025). Despite these achievements, however, clinical practice, particularly for complex chronic conditions (e.g., heart failure, HF), often depends on multimodal data in diagnosis, prognosis, and treatment (Weintraub 2019). This underscores the importance of multimodal strategies that go beyond language to support clinical practice.

While vision-language models (VLMs) such as LLaVA-Med (Li et al. 2023) and MedGemma (Sellersgren et al. 2025) have fueled anticipation for medical multimodal artificial intelligence (AI), several challenges remain. For example, they are restricted to static images, whereas dynamic inputs such as echocardiograms are vital for cardiac function assessment. In addition, such generalist models retain static knowledge, which hinders their ability to assimilate evolving medical evidence. While Retrieve-Augmented Generation (RAG) mitigates this challenge to some extent, traditional retrieval methods like Term Frequency-Inverse Document Frequency (TF-IDF) and dense passage retrieval (DPR) might be limited in semantic comprehension and retrieval relevance (Karpukhin et al. 2020; Mallen et al. 2023).

And most importantly, complex cardiovascular management often requires multi-step reasoning and a sequence of clinical actions, rather than a single-step response (McDonagh et al. 2021). Although prompt engineering techniques such as Chain-of-Thought (CoT) (Wei et al. 2022) partially mitigate this constraint by decomposing problems into sub-steps, model performance remains bounded by their intrinsic capabilities. The introduction of function calling and the Model Context Protocol (MCP) (Hou et al. 2025) provides solutions, which enables models to integrate external tools

automatically and access standardized functions. These advances drive the development of AI agents (Chang et al. 2024) capable of reasoning, planning, memory utilization, and action execution. However, most VLM-based agents in medicine still rely primarily on internal model knowledge and attempt to handle clinical tasks through one-hop question answering (Li et al. 2024) or role assignment (Kim et al. 2024).

Building upon recent efforts, MedAgent-Pro (Wang et al. 2025) proposes a solution for disease-level plan generation and patient-level reasoning. Nevertheless, its planning is conducted prior to receiving patient-specific input, while effective in some tasks, may lead to misalignment with individualized clinical contexts. For example, tasks for echocardiogram view identification typically follows a fixed workflow (e.g., commercial software, manual view selection), whereas complex HF diagnosis involves diverse patient presentations that require tailored test orders (e.g., ECG, echocardiography) and subsequent personalised management based on results. These highlight the need for flexible frameworks capable of both task-level and case-level adaptation across diverse clinical contexts. Another limitation of current VLM agents is the absence of intermediate visual outputs, such as delineation of the left ventricular contour, which are critical for clinical verification in complex or uncertain cases.

In this study, an adaptive framework, CardAIC-Agents, was introduced to augment models with external tools, enabling autonomous execution of cardiac tasks (e.g., diagnosis, echocardiogram view extraction, segmentation, detection of P, QRS, and T waves) across diverse modalities (e.g., tabular, textual, signal, image, and video). Specifically, the CardiacRAG agent was developed to formulate general plans based on the latest domain knowledge, whereas the chief agent enhanced its own capabilities through the integration and orchestration of external tools for plan execution and definitive decision-making. To support adaptive planning across tasks and patient-specific cases, the system initially assessed task complexity, executed the plan, and dynamically refined it as new evidence emerged. For more challenging cases, a multidisciplinary discussion tool was proposed to support further interpretation, where expertise across diverse modalities was integrated to fully explore information within the data. Finally, when clinicians raised concerns, visual review panels were provided for validation.

Experiments were conducted to evaluate the CardAIC-Agents in three public datasets, and the results indicated that its performance outperformed mainstream VLMs, state-of-the-art baseline agents, and fine-tuned VLMs specifically designed for the task. In addition, ablation studies verified the impact of key components. Finally, additional functionalities, such as echocardiogram view identification, were assessed by two cardiologists to show its applicability. In summary, the key contributions can be articulated as follows:

- A domain-specific framework, CardAIC-Agents, was developed to enhance the capabilities of large models through integration with specialized tools, facilitating autonomous execution of diverse cardiac tasks on multi-modal data.

- A CardiacRAG agent was introduced based on a novel hybrid retrieval method to extract relevant knowledge from an updated cardiac-specific resource base, enabling the formulation of clinical management plans and facilitation of adaptive clinical workflows.
- Adaptive strategies were proposed to stratify task complexity, refine plans, trigger multidisciplinary discussions for complex cases, and visually validate disputed cases, thereby enabling hierarchical adaptation tailored to specific clinical tasks and patients.

Related Work

Retrieve-Augmented Generation (RAG)

RAG is a technique that combines retrieval and generation to enhance text generation quality and relevance (Lewis et al. 2020). Unlike current LLMs such as GPT-3 (Brown et al. 2020), which possess strong generative capabilities but rely on internal knowledge that requires retraining to be updated, RAG could dynamically integrate external knowledge to generate timely and context-aware responses. Traditional retrieval methods, such as Term Frequency-Inverse Document Frequency (TF-IDF), assess document relevance based on keyword frequency, adjusted for document length and term distribution across the corpus (Aizawa 2003). While effective for lexical matching, its ability to capture semantic meaning is limited. Dense Passage Retrieval (DPR) is another semantic retrieval method that encodes queries and documents into high-dimensional embeddings (Karpukhin et al. 2020). However, such similarity-based approaches may still retrieve irrelevant results in certain cases (Mallen et al. 2023). In response to these limitations, this work proposed a hybrid retrieval approach that leverages both TF-IDF and DPR to enhance retrieval precision and contextual relevance.

AI Agents

The AI agent refers to a system that can perform goal-oriented tasks autonomously such as reasoning, planning, memory utilization, and action execution (Chang et al. 2024). LLM- and VLM-based agent frameworks, such as XAgent (2023) and MetaGPT (Hong et al. 2024), have shown the ability to decompose complex goals into sub-tasks and delegate them to specialized agents. In medical settings, LLMs with multi-agent collaboration (Tang et al. 2024; Chen, Saha, and Bansal 2024) are increasingly emphasized for complex clinical decisions; however, the lack of external tool integration limits them to relying solely on their intrinsic capabilities. Although the VLM-based MedAgent-Pro (Wang et al. 2025) augments its capabilities with external tools, it performs task-level planning prior to patient-specific input, which may constrain workflows and lead to misalignment with individual patient conditions. The ReAct-based framework (Yao et al. 2023), implemented in LangChain, performs iterative reasoning informed by prior outcomes to direct tool invocation, whereas constraints on input content and limitations in VLM guidance frequently result in redundant or suboptimal tool utilization.

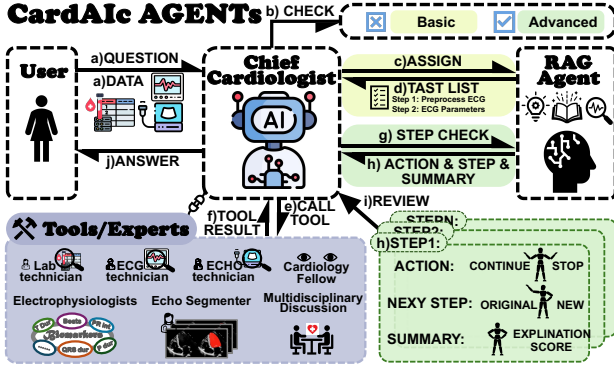


Figure 1: Overview of the CardAIC-Agents framework, where the RAG agent refers to the CardiacRAG agent, and the CardiacExperts agent comprises the chief cardiologist and diverse tool experts.

Method

CardAIC-Agents consisted of two components: the CardiacExperts agent and the CardiacRAG agent. The former included a chief cardiologist as well as tool experts from different specialties, where the chief cardiologist served as the primary decision-maker, responsible for determination of case complexity, task assignment, plan execution, and autonomous invocation of tools. The CardiacRAG agent, based on a dedicated cardiac knowledge base, generated and updated plans as new evidence emerged. An overview of the CardAIC-Agents framework is shown in Figure 1.

CardiacRAG Agent

The CardiacRAG agent was developed as current LLMs and VLMs encode static knowledge and their general-purpose design may lack cardiovascular domain specificity. This agent emulated the clinician reasoning process through information retrieval from authoritative medical sources and it was structured into three key stages (see Figure 2).

Knowledge base construction. To reduce the complexity of information retrieval and improve accuracy, the knowledge base construction process focused exclusively on cardiac content. This domain-specific approach selectively aggregated data $\{D_i\}_{i=1}^M = \{D_1, D_2, \dots, D_M\}$ from authoritative medical sources, including major US academic medical centers (e.g., Mayo Clinic (2025)), UK National Health Service (2025)), reputable health information platforms (e.g., MedlinePlus (2000)), and the most recently published official clinical guidelines. See Appendix A for more details.

Then, the raw documents $\{D_i\}_{i=1}^M$ were preprocessed through a transformation function T that extracts and normalizes textual content, producing clean text:

$$\{S_i\}_{i=1}^M = T(\{D_i\}_{i=1}^M), \quad i = 1, 2, \dots, M,$$

where T refers to BeautifulSoup (Abodayeh et al. 2023) for HTML files and Docling (Livathinos et al. 2025) for PDF files, and M refers to the total number of collected documents.

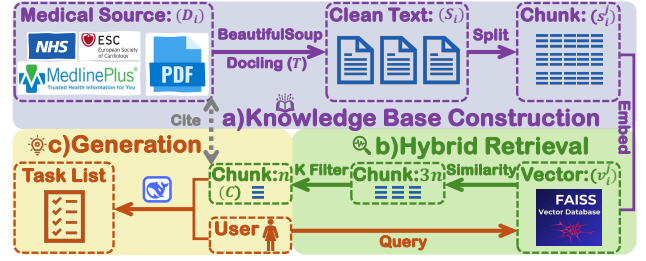


Figure 2: Illustration of the CardiacRAG agent. D_i denotes the i -th source, S_i is the cleaned text, s_i^j is the j -th chunk from source i , v_i^j is its corresponding vector, T represents the transfer method, K denotes keyword-based filtering, n is the number of chunks retrieved, c is the final retrieved content, and *Cite* indicates optional return of original chunks for transparency and reference.

Lastly, the texts were partitioned into overlapping chunks s_i^j to preserve contextual continuity:

$$s_i^j = \text{chunk}_j(S_i; d_s, d_o), \quad j = 1, 2, \dots, L_i,$$

where L_i denotes the total number of chunks generated from document i , j indexes the chunk position within document i , and d_s and d_o represent the chunk size and overlap size, respectively. Both were hyperparameters in this work.

Hybrid retrieval. To reduce irrelevant results from current vector similarity retrieval techniques, a hybrid retrieval method combined with a TF-IDF variants was applied to further filter results with domain-specific keyword, ensuring semantic relevance and clinical specificity.

- **Vector similarity retrieval:** to preserve semantic relevance, both chunks s_i^j and the query were embedded via Bio.ClinicalBERT (Alsentzer et al. 2019) as $v_i^j = \phi(s_i^j)$ and $q = \phi(\text{query})$. The complete set of document vectors ($\mathcal{V} = \bigcup_{i=1}^M \{v_i^j\}_{j=1}^{L_i}$) ranked by cosine similarity:

$$\text{sim}(q, v_i^j) = \frac{q \cdot v_i^j}{\|q\| \|v_i^j\|}, \quad (1)$$

and returned the top $3n$ vectors ($\mathcal{V}_{(1)}, \dots, \mathcal{V}_{(3n)}$), where n is the final number of results. Note that document vectors were indexed and stored in the FAISS vector database for efficient retrieval and reused without recalculation in subsequent queries.

- **Keyword-based filtering:** to improve clinical relevance, top $3n$ documents were further filtered based on domain-specific weights:

$$MW(k) = \begin{cases} \omega_{\text{medical}}[k], & k \in \mathcal{B}_{\text{medical}} \\ 1, & \text{otherwise} \end{cases}, \quad (2)$$

where k is a query keyword (Q), $\mathcal{B}_{\text{medical}}$ is the clinical vocabulary, and ω_{medical} is term importance. To exploit structural cues, a position-based bonus was introduced:

$$PB(k, s_i^j) = \begin{cases} 1.2, & \text{if } \text{pos}(k, s_i^j) < 0.3 \times |d_s| \\ 1, & \text{otherwise} \end{cases}, \quad (3)$$

where $\text{pos}(k, s_i^j)$ is the first occurrence index of k in chunk s_i^j , and $|d_s|$ is the chunk size. The final score was

$$\text{Score}_{(s_i^j, Q)} = \frac{1}{|Q|} \sum_{k \in Q} TF(k, s_i^j) \cdot MW(k) \cdot PB(k, s_i^j), \quad (4)$$

where chunks with scores above threshold θ were retained, and term frequency defined as:

$$TF(k, s_i^j) = \frac{\text{count}(k, s_i^j)}{|\text{words}(s_i^j)|}. \quad (5)$$

Guideline generation. Based on the retrieved chunks $C = \{c_1, c_2, \dots, c_n\}$, an LLM generated a general plan P for the query. For complex cases, this plan could be continuously updated as new results become available during subsequent steps, thereby better reflecting real-world clinical practices.

- **General plan:** given the retrieved context C , the LLM generated a procedural plan P defined as an ordered sequence of steps:

$$P = \text{LLM}(\text{Prompt}(Q, C)),$$

where Prompt formats the input query Q and the context C into a template tailored for procedural guidance generation. DeepSeek-R1-Distill-Qwen-32B (DeepSeek-AI 2025) was employed as the LLM. The plan $P = (p_1, p_2, \dots, p_s)$ contained s steps, which could vary by case.

- **Stepwise update:** at each step s , the following process was applied:

$$(S, A, P_{s+1}) = \text{DeepSeek-R1}(P_s, t_s),$$

where S is the summary of results accumulated so far, A is the action indicator (whether to stop or continue), and P_{s+1} is the next step in the plan. P_{s+1} returns null if no update is needed, or the modified plan if an update occurs.

CardiacExperts Agent

The CardiacExperts agent employed an LLM as the chief cardiologist and orchestrated multiple specialized tools as domain experts to collectively support cardiac tasks.

Chief cardiologist. It leveraged advanced reasoning capabilities of the LLM to assess the task complexity, assign it to the CardiacRAG agent for planning, execute these plans, and autonomously coordinate and invoke appropriate tools. Once a task was identified as complex, the CardiacRAG agent would continuously review and update the plan based on intermediate results, deciding whether to modify, stop, or continue the workflow. Upon completion of all steps, the chief cardiologist questioned and evaluated the completed steps and its results, and then provided the final decision along with a summary and answer, formulated as:

$$(\text{Summary}, \text{Answer}) = \text{DeepSeek-R1}(P, t).$$

Tools. These tools acted as experts in their specific domains.

- **Laboratory technician:** this tool preprocesses laboratory test results (Labs, tabular data) for downstream analysis by extracting clinical information such as demographics, laboratory values, and medication history from structured or semi-structured text, producing both natural language outputs and their tokenized representations.

$$(Lab_{\text{text}}, Lab_{\text{token}}) = \text{LabProcessor}(\text{Labs}).$$

- **ECG technician:** this tool preprocesses raw 12-lead electrocardiogram signals (ECGs) through bandpass filtering, noise removal, and baseline drift correction to support downstream analysis, and also extracts quantitative parameters such as mean amplitude and standard deviation.

$$(\text{ECG}_{\text{text}}, \text{ECG}_{\text{signal}}) = \text{ECGProcessor}(\text{ECGs}).$$

- **Electrophysiologists:** this functionality is implemented with NeuroKit2, a Python toolbox, to obtain 12-leads ECG measurements, include signal quality scores, heart rate variability (HRV) features, wave durations (e.g., QRS, PR, QT intervals), and extract heartbeat images from representative leads (e.g., I, II, III, and V5).

$$(\hat{E}, \hat{B}) = \text{NeuroKit2}(\text{ECGs}),$$

where $\hat{E} = \{\hat{e}_1, \hat{e}_2, \dots, \hat{e}_m\}$ represents the extracted ECG measurements, and $\hat{B} = \{\hat{b}_I, \hat{b}_{II}, \hat{b}_{V5}\}$ denotes the extracted heartbeat images from the respective leads.

- **Echocardiography technician:** this tool functions as a view classifier (Vukadinovic et al. 2024) to extract standard cardiac views, including apical two-chamber (A2C), apical three-chamber (A3C), apical four-chamber (A4C), apical five-chamber (A5C), apical Doppler (AD), colour Doppler parasternal long-axis (DPL), colour Doppler parasternal short-axis (DPS), parasternal long-axis (PSL), parasternal short-axis (PSS), suprasternal short-axis (SSN), and subcostal view (Sub), from raw DICOM data:

$$\text{View} = \text{ViewClassifier}(\text{DICOM}).$$

- **Echocardiography segmenter:** this tool performs segmentation for echocardiograms (ECHOs), which is essential for tracking cardiac function in clinical practice. Here, a segmentation network (Zhang et al. 2024) was employed to generate pixel-wise masks (Mask) to delineate cardiac structures in apical four-chamber videos (EchoVideo_{A4c}):

$$\text{Mask} = \text{SegNetwork}(\text{EchoVideo}_{A4c}).$$

- **Cardiology fellow:** a fine-tuned multimodal model is employed for preliminary disease diagnosis (Y) based on diverse data modalities:

$$Y = \text{TGMM}(\text{Labs}, \text{ECGs}, \text{ECHOs}).$$

- **Multidisciplinary discussion:** this team reviews raw inputs and intermediate outputs (e.g., heartbeat images from electrophysiologists) to support comprehensive decisions. Firstly, the chief cardiologist designates two relevant domain expert roles based on the query. Each expert analyzes the inputs independently, and their individual results are synthesized by the chief. Then, the two experts review this synthesis along with intermediate outputs from other tools, after which the chief cardiologist re-synthesizes the updated information. When the two experts reach consensus or the maximum number of predefined discussion rounds (hyperparameter) is exhausted, the chief issues the final decision. Note that the two experts were implemented based on MedGemma from Google (Sellergren et al. 2025), which is specialized for medical image analysis, and Qwen2.5-VL from Alibaba (Bai et al. 2023), which excels at video processing. The discussion process consists of $T/2$ rounds:

$$\left\{ \begin{array}{l} Q_1 = \text{Qwen}(I), \quad P_1 = \text{MedGemma}(I), \\ D_1 = \text{DeepSeek-R1}(Q_1, P_1), \\ Q_2 = \text{Qwen}(D_1, Z), \quad P_2 = \text{MedGemma}(D_1, Z), \\ D_2 = \text{DeepSeek-R1}(Q_2, P_2), \\ \text{for } t = 3, 4, \dots, T : \\ \quad \left\{ \begin{array}{l} \text{if } t \text{ odd:} \\ \quad Q_t = \text{Qwen}(D_{t-1}, I), P_t = \text{MedGemma}(D_{t-1}, I), \\ \text{if } t \text{ even:} \\ \quad Q_t = \text{Qwen}(D_{t-1}, Z), P_t = \text{MedGemma}(D_{t-1}, Z), \\ \quad D_t = \text{DeepSeek-R1}(Q_t, P_t), \\ \text{if } (\text{agree}(Q_t, D_{t-1}) \wedge \text{agree}(P_t, D_{t-1})) \vee (t = T) : \\ \quad \text{stop iteration.} \end{array} \right. \end{array} \right.$$

where T is the total number of reasoning steps, I is the original input, Z denotes intermediate outputs from other expert tools, and Q_*, P_*, D_* are the responses from models. Note that the raw input I and auxiliary data Z were reintroduced in subsequent iterations to mitigate error propagation from model hallucinations.

Experiments

Experimental Settings

Datasets. The performance of CardAIC-Agents was evaluated on three publicly multimodal datasets related to cardiac care: (i) MIMIC-IV (Johnson et al. 2023), for HF diagnosis, which includes data from 1,524 patients with three modalities: laboratory test results (Labs), 12-lead electrocardiogram (ECGs), and echocardiograms (ECHOs); (ii) PTB-XL (Wagner et al. 2020) and its extended version PTB-XL+ for Myocardial infarction (MI) diagnosis (Strodthoff et al. 2023), comprising data from 10,147 patients, with two modalities: structured patient information and ECG-derived features, and 12-lead ECGs; (iii) PTB diagnostic ECG database for external validation of HF prediction, containing data with 268 cases and two modalities: patient information and 12-lead ECGs. Further details were provided in Appendix B.

Metrics. The diagnostic performance was evaluated with accuracy-based metrics, including the area under the receiver operating characteristic curve (AUC) and overall accuracy (Yu et al. 2021), with 95% confidence intervals. For the intermediate visual outputs, two cardiologists independently assessed and scored the results.

Baseline. The proposed agent was evaluated against medical VLMs, including LLaVA-Med from Microsoft (Li et al. 2023) and MedGemma from Google (Sellergren et al. 2025). To assess current step-by-step reasoning and tool-augmented strategies, MedGemma combined with CoT (Wei et al. 2022) and ReAct (Yao et al. 2023) was also included. In addition, comparisons were conducted with advanced medical agent systems, such as MedAgents (Tang et al. 2024), ReConcile (Chen, Saha, and Bansal 2024), and MDAgents (Kim et al. 2024). Furthermore, fine-tuned VLMs developed for specific tasks were also evaluated, including Qwen2.5-VL from Alibaba (Bai et al. 2023) and Janus-Pro from Deepseek AI (Chen et al. 2025). Note that, as some models did not support for ECG or video inputs, these modalities were transformed into compatible formats (e.g., text or image) to ensure a fair comparison. More implementation details were provided in Appendix C.

Results and Comparative Analysis

Comparison with VLMs and variants. As shown in Table 1, CardAIC-Agents outperformed all baseline VLMs across the three cardiac datasets. The most significant performance gap was observed on the MIMIC-IV, where CardAIC-Agents achieved an accuracy of 0.87 compared to only 0.35 by LLaVA-Med ($p < 0.05$). This was partly due to the limited token input length, which constrained the performance of this medical yet general VLM. Secondly, MedGemma performed the best among the VLMs, while enabling CoT reasoning did not improve performance across all datasets. Finally, its ReAct system was built on LangChain to invoke tools, which improved performance on PTB-XL but not on MIMIC-IV. This disparity likely arised from the higher textual complexity in MIMIC-IV, which may challenge the VLM in language understanding and lead to redundant or ineffective tool invocations. In summary, the proposed agent outperformed existing general-purpose medical VLMs, even when external tools were included.

Comparison with medical agent. The proposed agent outperformed state-of-the-art medical agents across all datasets (Table 1). Among these, ReConcile showed the largest performance gap, with accuracies of 0.49 (vs. 0.87) on MIMIC-IV, 0.43 (vs. 0.96) on PTB-XL, and 0.55 (vs. 0.77) on PTB Diagnostic ($p < 0.05$). A key limitation of these agents lay in their reliance on the intrinsic capabilities of models; inference remained constrained despite guidance from predefined expert-role prompts. In addition, their static knowledge bases might limit adaptability. Moreover, the sequential nature of their reasoning pipelines could propagate early errors or hallucinations, leading to compounding flaws. By contrast, the proposed agent leveraged an up-to-date CardiacRAG agent, integrated external tools to augment model capabilities, and incorporated reflective mecha-

Table 1: Performance Comparison across Methods and Datasets

Category	Method	MIMIC-IV		PTB-XL		PTB Diagnostic	
		ACC	AUC	ACC	AUC	ACC	AUC
VLMs & Variants	LLaVA-Med (Li et al. 2023)	0.35 (0.30, 0.41)	0.34 (0.28, 0.40)	0.39 (0.37, 0.42)	0.51 (0.47, 0.55)	0.12 (0.08, 0.16)	0.44 (0.34, 0.59)
	MedGemma (Sjellgren et al. 2025)	0.76 (0.71, 0.80)	0.82 (0.77, 0.86)	0.56 (0.53, 0.59)	0.55 (0.52, 0.59)	0.76 (0.71, 0.81)	0.88 (0.83, 0.93)
	MedGemma (CoT) (Wei et al. 2022)	0.65 (0.60, 0.70)	0.81 (0.76, 0.86)	0.53 (0.50, 0.56)	0.54 (0.50, 0.58)	0.58 (0.52, 0.64)	0.75 (0.64, 0.88)
	MedGemma (ReAct) (Yao et al. 2023)	0.67 (0.62, 0.72)	0.71 (0.66, 0.76)	0.83 (0.81, 0.85)	0.83 (0.80, 0.85)	0.69 (0.64, 0.75)	0.72 (0.41, 0.99)
Medical Agents	MedAgents (Tang et al. 2024)	0.74 (0.70, 0.79)	0.82 (0.78, 0.87)	0.65 (0.62, 0.68)	0.62 (0.58, 0.66)	0.75 (0.70, 0.79)	0.84 (0.74, 0.92)
	ReConcile (Chen, Saha, and Bansal 2024)	0.49 (0.44, 0.55)	0.75 (0.69, 0.80)	0.43 (0.40, 0.46)	0.57 (0.53, 0.61)	0.55 (0.49, 0.61)	0.76 (0.58, 0.93)
	MDAgents (Kim et al. 2024)	0.52 (0.47, 0.58)	0.61 (0.55, 0.68)	0.56 (0.52, 0.58)	0.60 (0.56, 0.64)	0.74 (0.68, 0.79)	0.74 (0.53, 0.96)
Fine-tuned VLMs	Qwen2.5-VL (Bai et al. 2023)	0.78 (0.73, 0.82)	0.85 (0.81, 0.90)	0.93 (0.91, 0.94)	0.96 (0.94, 0.97)	0.72 (0.66, 0.77)	0.80 (0.61, 0.99)
	Janus-Pro (Chen et al. 2025)	0.84 (0.79, 0.88)	0.91 (0.88, 0.94)	0.96 (0.95, 0.97)	0.99 (0.98, 0.99)	0.75 (0.70, 0.80)	0.83 (0.57, 0.99)
Proposed	CardAIC-Agents	0.87 (0.82, 0.90)	0.89 (0.85, 0.93)	0.96 (0.95, 0.97)	0.96 (0.94, 0.98)	0.77 (0.72, 0.82)	0.88 (0.65, 1.00)

Note: Underlined values indicate best performance within each dataset and metric; Values in parentheses represent 95% confidence intervals; ACC = accuracy; AUC = Area Under the Curve; CoT = Chain of Thought; ReAct = Reasoning and Acting.

Table 2: Ablation Study of Key Components

Components			Performance	
RAGAgent	Step	Team	ACCURACY	AUC
	✓	✓	0.77(0.72,0.82)	0.81(0.76,0.86)
✓		✓	0.80(0.75,0.85)	0.87(0.83,0.91)
✓	✓		0.84(0.80,0.88)	0.88(0.84,0.92)
✓	✓	✓	0.87(0.83,0.90)	0.89(0.85,0.93)

Note: ✓ indicates component enabled; Underlined values indicate best performance; Values in parentheses represent 95% confidence intervals;

nisms that continuously revisit prior reasoning steps as well as inputs, thereby reducing error accumulation.

Comparison with fine-tuned VLMs. The proposed agent achieved performance comparable to that of fine-tuned VLMs specifically optimized for their respective tasks. The results showed that it outperformed Qwen2.5-VL across all three datasets and achieved performance comparable to Janus-Pro on the first two datasets. To assess generalization, all fine-tuned models were directly evaluated on the PTB Diagnostic Database for HF diagnosis without any task-specific adaptation (see Table 1). The results showed that Qwen2.5-VL and Janus-Pro achieved accuracies of 0.72 and 0.75, respectively (vs. 0.77, $p < 0.05$). Another finding was that the fine-tuned Janus-Pro achieved a higher AUC than the proposed agent on the first two datasets. This difference might have stemmed from the tendency of LLM-based agents to assign elevated baseline probabilities even in the absence of explicit diagnoses, whereas fine-tuned models typically generated more precise probability estimates, often benefiting from higher numerical precision (e.g., 16- or 32-bit).

Assessment of intermediate visual outputs. CardAIC-Agents could also provide on-demand support to clinicians for the validation of complex or uncertain cases; therefore, a review panel was introduced to facilitate this process, as shown in Figure 3. This function was evaluated in collaboration with two cardiologists. For echocardiography, the agent automatically identified 11 standard views from raw DICOM images, achieving 100% accuracy in key views (e.g., A3C, A4C, PLAX, PSAX, SC) and over 80% accuracy in others (based on a random sample of 10 cases); Left ventri-

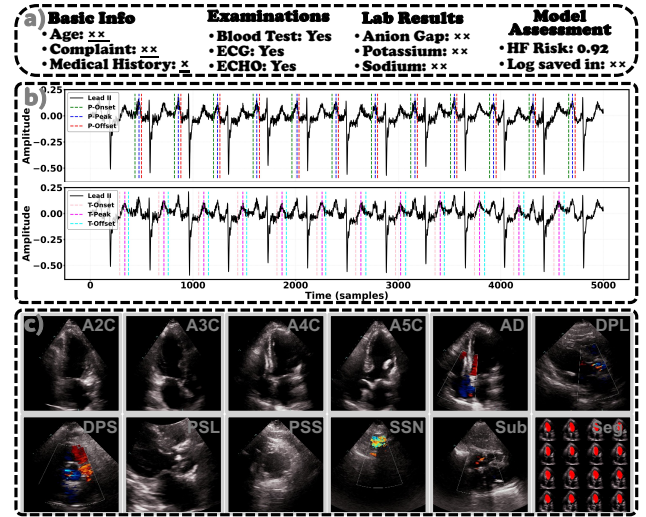


Figure 3: Review Panel: (a) patient profile display; (b) ECG waveform with labeled P and T waves; (c) echocardiographic view identification and A4C segmentation (Seg.).

cle segmentation on A4C views had been reported by original studies with a Dice coefficient of 0.922 on the EchoNet-Dynamic dataset. In addition, detection of P, QRS, and T waves from 12-lead ECGs was rated suboptimal by clinical experts, mainly due to stringent criteria requiring precise identification of every heartbeat, indicating a key area for further improvement. Note that Figure 3 presents only partial results, with additional details provided in the Appendix.

Ablation Studies

CardiacRAG agent. The ablation study was conducted on the MIMIC-IV dataset to evaluate the contribution of CardiacRAG agent (see Table 2). The results showed a clear improvement when a dedicated and independent agent was assigned to generate and refine plans based on domain knowledge, yielded a 10% performance improvement. This highlighted the effectiveness of the proposed module in precisely retrieving relevant information, as well as the valuable contribution of its curated domain-specific knowledge base.

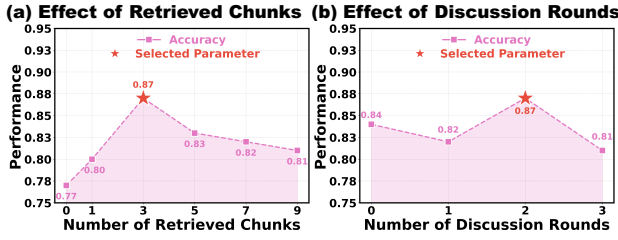


Figure 4: Hyperparameter selection on the MIMIC-IV.

Adaptive step-wise inference. The contribution of adaptive step-wise inference was shown in Table 2, where accuracy improved from 0.80 to 0.87 ($p < 0.05$). This result confirmed the effectiveness of reasoning in an incremental, feedback-aware manner. Specifically, the model performed step-by-step evaluation and summarization, allowing it to reassess the current state at each stage and adjust the plan accordingly before proceeding. This process not only adapted flexibly to cases but also reduced the risk of error propagation by enabling the system to detect and correct earlier mistakes, rather than compounding them in subsequent reasoning steps.

Multidisciplinary discussion. Table 2 also reported an increase from 0.84 to 0.87 attributed to the proposed multidisciplinary discussion team ($p < 0.05$). This improvement reflected two key drivers: first, the effectiveness of this tool to incorporate diverse multimodal information and assign distinct roles to specialized models for collaborative discussion; second, the capability of the agent to dynamically activate the tool upon detecting uncertainty or insufficient evidence in earlier reasoning stages, selectively engaging the team as needed. Such improvement also confirmed the benefits of the proposed hierarchical adaptation strategy.

Parameter Analysis

Furthermore, the analysis was extended to assess the sensitivity of two key parameters: the number of retrieved chunks and the maximum number of rounds allowed for the multidisciplinary discussion (see Figure 4). MIMIC-IV was used as a typical example for this analysis. The results indicated that increasing the number of retrieved chunks initially improved performance, peaking at three chunks. Beyond this point, performance declined. This trend could be attributed to two factors: when too few knowledge chunks were available, the model lacked sufficient context to make informed decisions; however, when the number exceeded a certain threshold, the input might have surpassed the effective token processing capacity of the model, which degraded performance. Similarly, the analysis revealed that the best accuracy was achieved with two rounds of discussion. Both fewer and more rounds resulted in performance below the baseline (i.e., without the discussion tool). This highlighted the importance of carefully tuning the number of discussion rounds, as suboptimal settings could lead to unreliable intermediate reasoning and potentially misguide the final decision made by the chief cardiologist.

Limitations

While the CardAIC-Agents showed competitive performance across three dataset, several limitations remained. First, the absence of labeled visual panel information (e.g., DICOM view labels) limited the ability to systematically and quantitatively assess this functionality, though visual validation by cardiologists was conducted to partially mitigate this limitation. Second, its AUC remained lower than that of fine-tuned models, even though this gap might have been attributable to the coarse-grained prediction precision inherent to LLM outputs; nevertheless, the agent showed notable accuracy gains, highlighting its potential for early screening, for example, in resource-limited settings. In light of these challenges, future research would prioritize precision medicine applications in clinical practice.

Conclusion

This study introduced CardAIC-Agents, a multimodal framework designed with adaptive capabilities for cardiac-related tasks. Experiments on three public datasets showed that it outperformed general medical VLMs and state-of-the-art medical agents, and was comparable to fine-tuned models. In summary, this study, combined with external tools and cardiac-related knowledge base, presented a hierarchical adaptive framework, from complexity assessment and iterative plan refinement as new evidence emerges, through dynamic activation of specialized team discussions for complex cases, to the provision of visual outputs to support clinicians in further verification. With this adaptive design, CardAIC-Agents offered a viable solution for early detection in resource-limited clinical settings.

References

- Abodayeh, A.; Hejazi, R.; Najjar, W.; Shihadeh, L.; and Latif, R. 2023. Web scraping for data analytics: A beautiful-soup implementation. In *Sixth International Conference of Women in Data Science at Prince Sultan University (WiDS PSU)*, 65–69. Riyadh, Saudi Arabia: Institute of Electrical and Electronics Engineers Inc.
- Aizawa, A. 2003. An information-theoretic perspective of tf-idf measures. *Information Processing & Management*, 39(1): 45–65.
- Almeida, A. G.; Grapsa, J.; Gimelli, A.; Bucciarelli-Ducci, C.; Gerber, B.; Ajmone-Marsan, N.; Bernard, A.; Donal, E.; Dweck, M. R.; Haugaa, K. H.; et al. 2024. Cardiovascular multimodality imaging in women: a scientific statement of the European Association of Cardiovascular Imaging of the European Society of Cardiology. *European Heart Journal-Cardiovascular Imaging*, 25(4): e116–e136.
- Alsentzer, E.; Murphy, J.; Boag, W.; Weng, W.-H.; Jindi, D.; Naumann, T.; and McDermott, M. 2019. Publicly Available Clinical BERT Embeddings. In *Proceedings of the 2nd Clinical Natural Language Processing Workshop (ClinicalNLP)*, 72–78. Minneapolis, USA: Association for Computational Linguistics.
- Bai, J.; Bai, S.; Yang, S.; Wang, S.; Tan, S.; Wang, P.; Lin, J.; Zhou, C.; and Zhou, J. 2023. Qwen-VL: A Versatile Visi

- on-Language Model for Understanding, Localization, Text Reading, and Beyond. *arXiv:2308.12966*.
- Brin, D.; Sorin, V.; Vaid, A.; Soroush, A.; Glicksberg, B. S.; Charney, A. W.; Nadkarni, G.; and Klang, E. 2023. Comparing ChatGPT and GPT-4 performance in USMLE soft skill assessments. *Scientific Reports*, 13(1): 16492.
- Brown, T.; Mann, B.; Ryder, N.; Subbiah, M.; Kaplan, J. D.; Dhariwal, P.; Neelakantan, A.; Shyam, P.; Sastry, G.; Askell, A.; et al. 2020. Language models are few-shot learners. In *Proceedings of the 34th International Conference on Neural Information Processing Systems (NeurIPS)*, 1877–1901. Vancouver, Canada: Curran Associates, Inc.
- Bulto, L. N.; and Hendriks, J. M. 2024. The burden of cardiovascular disease in Africa: prevention challenges and opportunities for mitigation. *European Journal of Cardiovascular Nursing*, 23(6): e88–e90.
- Chang, M.; Zhang, J.; Zhu, Z.; Yang, C.; Yang, Y.; Jin, Y.; Lan, Z.; Kong, L.; and He, J. 2024. Agentboard: An analytical evaluation board of multi-turn llm agents. In *Proceedings of the 38th International Conference on Neural Information Processing Systems (NeurIPS)*, 74325–74362. Vancouver, Canada: Curran Associates.
- Chen, J.; Saha, S.; and Bansal, M. 2024. ReConcile: Round-Table Conference Improves Reasoning via Consensus among Diverse LLMs. In *Proceedings of the 62nd Annual Meeting of the Association for Computational Linguistics (ACL)*, 7066–7085. Bangkok, Thailand: Association for Computational Linguistics.
- Chen, X.; Wu, Z.; Liu, X.; Pan, Z.; Liu, W.; Xie, Z.; Yu, X.; and Ruan, C. 2025. Janus-pro: Unified multimodal understanding and generation with data and model scaling. *arXiv:2501.17811*.
- DeepSeek-AI. 2025. DeepSeek-R1: Incentivizing Reasoning Capability in LLMs via Reinforcement Learning. *arXiv:2501.12948*.
- Hong, S.; Zhuge, M.; Chen, J.; Zheng, X.; Cheng, Y.; Wang, J.; Zhang, C.; Wang, Z.; Yau, S.; Lin, Z.; Zhou, L.; Ran, C.; Xiao, L.; Wu, C.; and Schmidhuber, J. 2024. MetaGPT: Meta Programming for a Multi-Agent Collaborative Framework. In *Proceedings of the International Conference on Representation Learning (ICLR)*, 23247–23275. Vienna, Austria: ICLR Organization.
- Hou, X.; Zhao, Y.; Wang, S.; and Wang, H. 2025. Model context protocol (mcp): Landscape, security threats, and future research directions. *arXiv:2503.23278*.
- Johnson, A. E.; Bulgarelli, L.; Shen, L.; Gayles, A.; Sham-mout, A.; Horng, S.; Pollard, T. J.; Hao, S.; Moody, B.; Gow, B.; et al. 2023. MIMIC-IV, a freely accessible electronic health record dataset. *Scientific data*, 10(1): 1.
- Karpukhin, V.; Oguz, B.; Min, S.; Lewis, P.; Wu, L.; Edunov, S.; Chen, D.; and Yih, W.-t. 2020. Dense Passage Retrieval for Open-Domain Question Answering. In *Proceedings of the 2020 Conference on Empirical Methods in Natural Language Processing (EMNLP)*, 6769–6781. Online: Association for Computational Linguistics.
- Kim, Y.; Park, C.; Jeong, H.; Chan, Y. S.; Xu, X.; McDuff, D.; Lee, H.; Ghassemi, M.; Breazeal, C.; and Park, H. W. 2024. MDAgents: An Adaptive Collaboration of LLMs for Medical Decision-Making. In *Proceedings of the 38th International Conference on Neural Information Processing Systems (NeurIPS)*, 79410–79452. Vancouver, Canada: Curran Associates, Inc.
- Lewis, P.; Perez, E.; Piktus, A.; Petroni, F.; Karpukhin, V.; Goyal, N.; Küttler, H.; Lewis, M.; Yih, W.-t.; and Rocktäschel, T. 2020. Retrieval-augmented generation for knowledge-intensive NLP tasks. In *Proceedings of the 34th International Conference on Neural Information Processing Systems (NeurIPS)*, 9459–9474. Red Hook, USA: Curran Associates Inc.
- Li, B.; Yan, T.; Pan, Y.; Luo, J.; Ji, R.; Ding, J.; Xu, Z.; Liu, S.; Dong, H.; Lin, Z.; and Wang, Y. 2024. MMedAgent: Learning to Use Medical Tools with Multi-modal Agent. In *Findings of the Association for Computational Linguistics:EMNLP*, 8745–8760. Miami, USA: Association for Computational Linguistics.
- Li, C.; Wong, C.; Zhang, S.; Usuyama, N.; Liu, H.; Yang, J.; Naumann, T.; Poon, H.; and Gao, J. 2023. LLaVA-med: Training a large language-and-vision assistant for biomedicine in one day. In *Proceedings of the 37th International Conference on Neural Information Processing Systems (NeurIPS)*, 24. Red Hook, USA: Curran Associates Inc.
- Livathinos, N.; Auer, C.; Lysak, M.; Nassar, A.; Dolfi, M.; Vagenas, P.; Ramis, C. B.; Omenetti, M.; Dinkla, K.; Kim, Y.; et al. 2025. Docling: An Efficient Open-Source Toolkit for AI-Driven Document Conversion. In *Proceedings of the AAAI 2025 Workshop on Open-Source AI for Mainstream Use*. Philadelphia, USA: AAAI Press.
- Mallen, A.; Asai, A.; Zhong, V.; Das, R.; Khashabi, D.; and Hajishirzi, H. 2023. When Not to Trust Language Models: Investigating Effectiveness of Parametric and Non-Parametric Memories. In *Proceedings of the 61st Annual Meeting of the Association for Computational Linguistics (ACL)*, 9802–9822. Toronto, Canada: Association for Computational Linguistics.
- Mayo Foundation for Medical Education and Research. 2025. Mayo Clinic. <https://www.mayoclinic.org/>. Accessed: 2025-04-01.
- McDonagh, T. A.; Metra, M.; Adamo, M.; Gardner, R. S.; Baumbach, A.; Böhm, M.; Burri, H.; Butler, J.; Čelutkienė, J.; Chioncel, O.; et al. 2021. 2021 ESC Guidelines for the diagnosis and treatment of acute and chronic heart failure: Developed by the Task Force for the diagnosis and treatment of acute and chronic heart failure of the European Society of Cardiology (ESC) With the special contribution of the Heart Failure Association (HFA) of the ESC. *European heart journal*, 42(36): 3599–3726.
- Miller, N.; Lacroix, E.-M.; and Backus, J. E. 2000. MEDLINEplus: building and maintaining the National Library of Medicine’s consumer health Web service. *Bulletin of the Medical Library Association*, 88(1): 11.
- NHS. 2025. National Health Service. <https://www.nhs.uk/>. Accessed: 2025-04-01.
- Sellergren, A.; Kazemzadeh, S.; Jaroensri, T.; Kiraly, A.; Traverse, M.; Kohlberger, T.; Xu, S.; Jamil, F.; Hughes,

- C.; Lau, C.; et al. 2025. MedGemma Technical Report. *arXiv:2507.05201*.
- Singhal, K.; Tu, T.; Gottweis, J.; Sayres, R.; Wulczyn, E.; Amin, M.; Hou, L.; Clark, K.; Pfohl, S. R.; Cole-Lewis, H.; et al. 2025. Toward expert-level medical question answering with large language models. *Nature Medicine*, 31(3): 943–950.
- Strodthoff, N.; Mehari, T.; Nagel, C.; Aston, P. J.; Sundar, A.; Graff, C.; Kanters, J. K.; Haverkamp, W.; Dössel, O.; Loewe, A.; et al. 2023. PTB-XL+, a comprehensive electrocardiographic feature dataset. *Scientific data.*, 10(1): 279.
- Tang, X.; Zou, A.; Zhang, Z.; Li, Z.; Zhao, Y.; Zhang, X.; Cohan, A.; and Gerstein, M. 2024. MedAgents: Large Language Models as Collaborators for Zero-shot Medical Reasoning. In *Proceedings of Findings of the Association for Computational Linguistics (ACL)*, 599–621. Bangkok, Thailand: Association for Computational Linguistics.
- Vedanthan, R.; and Fuster, V. 2011. Urgent need for human resources to promote global cardiovascular health. *Nature Reviews Cardiology*, 8(2): 114–117.
- Vukadinovic, M.; Tang, X.; Yuan, N.; Cheng, P.; Li, D.; Cheng, S.; He, B.; and Ouyang, D. 2024. EchoPrime: A Multi-Video View-Informed Vision-Language Model for Comprehensive Echocardiography Interpretation. *arXiv:2410.09704*.
- Wagner, P.; Strodthoff, N.; Bousseljot, R.-D.; Kreiseler, D.; Lunze, F. I.; Samek, W.; and Schaeffter, T. 2020. PTB-XL, a large publicly available electrocardiography dataset. *Scientific data*, 7(1): 1–15.
- Wang, Z.; Wu, J.; Cai, L.; Low, C. H.; Yang, X.; Li, Q.; and Jin, Y. 2025. MedAgent-Pro: Towards Evidence-Based Multi-Modal Medical Diagnosis via Reasoning Agentic Workflow. *arXiv:2503.18968*.
- Wei, J.; Wang, X.; Schuurmans, D.; Bosma, M.; Xia, F.; Chi, E.; Le, Q. V.; Zhou, D.; et al. 2022. Chain-of-thought prompting elicits reasoning in large language models. In *Proceedings of the 36th Conference on Neural Information Processing Systems (NeurIPS)*, 24824–24837. New Orleans, USA: Curran Associates Inc.
- Weintraub, W. S. 2019. Role of big data in cardiovascular research. *Journal of the American Heart Association*, 8(14): e012791.
- XAgent Team. 2023. XAgent: An Autonomous Agent for Complex Task Solving. <https://github.com/OpenBMB/XAgent>. Accessed: 2025-04-01.
- Yao, S.; Zhao, J.; Yu, D.; Du, N.; Shafran, I.; Narasimhan, K.; and Cao, Y. 2023. React: Synergizing reasoning and acting in language models. In *Proceedings of the 11th International Conference on Learning Representations (ICLR)*. Kigali, Rwanda.
- Yu, H.; Deng, J.; Nathan, R.; Kröschel, M.; Pekarsky, S.; Li, G.; and Klaassen, M. 2021. An evaluation of machine learning classifiers for next-generation, continuous-ethogram smart trackers. *Movement Ecology*, 9: 1–14.
- Zhang, Y.; Liu, B.; Bunting, K. V.; Brind, D.; Thorley, A.; Karwath, A.; Lu, W.; Zhou, D.; Wang, X.; Mobley, A. R.; et al. 2024. Development of automated neural network prediction for echocardiographic left ventricular ejection fraction. *Frontiers in Medicine*, 11: 1354070.